

Enhancement of room-temperature photoluminescence in thin-film polycrystalline silicon produced by low power laser annealing

S. Ostapenko,^{a)} A. U. Savchuk,^{b)} G. Nowak, J. Lagowski,
and A. M. Hoff

Center for Microelectronics Research, University of South Florida, Tampa, Florida 33620

(Received 7 August 1995; accepted for publication 5 September 1995)

We have found that seconds of 100 mW Ar laser exposure produces more than 100 times an increase in infrared photoluminescence (PL) intensity in thin-film polycrystalline silicon (poly-Si). The change of PL intensity on laser exposed film areas (minimum spot size of 20 μm) and the variation in film surface morphology measured by atomic force microscope are compared. The effect of PL enhancement strongly correlates to two distinctive processes: (a) the increase of a grain size due to poly-Si recrystallization, and (b) the oxygen incorporation into the film from glass or quartz substrates or/and from ambient gas. © 1995 American Institute of Physics.

Light emission from silicon has been utilized as a sensitive spectroscopic tool for defect diagnostics,¹ while Si based materials have shown promise for optoelectronics, in particular, as light emitting devices.² The room-temperature photoluminescence (PL) in Si single crystals is rather weak with internal quantum efficiency on the order of $10^{-2}\%$.³ It is recognized that the application of silicon in light emitting devices demands a substantial enhancement of PL efficiency. In this concern, a recent discovery of intensive band-tail PL transitions in polycrystalline silicon (poly-Si) thin films on glass substrates (Ref. 4) makes this material promising for light emitting applications. In this letter, we report a new observation of the enhancement of room-temperature photoluminescence in poly-Si thin films due to low-power Ar laser annealing.

Undoped low pressure chemical vapor deposition (LPCVD) Si films with thickness from 0.45 to 0.55 μm were deposited at 550 or 625 °C on Corning 7059 glass or fused silica substrates. X-ray diffraction proved that 625 °C films had $\langle 110 \rangle$ oriented crystal structure, while the as-grown 550 °C films were amorphous. Subsequent prolonged annealing (8–75 h) of 550 °C deposited films in nitrogen at 600 °C caused a gradual development of the $\langle 111 \rangle$ polycrystal structure. Prior to laser processing all samples were dipped in a 10% HF/DI water solution for a few seconds to remove any native oxide from the film surface. Photoluminescence was analyzed using a single SPEC 500M spectrometer coupled with a liquid nitrogen cooled Ge detector or, alternatively, with PbS detector cooled with dry ice. PL spectra were corrected for the spectral response of the setup. The 514 nm Ar^+ laser line with power ranging from 60 to 280 mW was used as the PL excitation source. For laser annealing, the same 514 nm laser line focused by a 110 mm lens at a 20 μm spot provided the power density up to 10^5 W/cm^2 . The absorption coefficient of poly-Si films at 514 nm, evaluated from room-temperature transmission data, is $3 \times 10^4 \text{ cm}^{-1}$. The PL setup allows luminescence mapping by scanning the excitation laser beam with the smallest step of 1 μm . The

lateral resolution of the mapping system was limited only by the Ar laser spot size (20 μm). The surface topography of untreated and laser processed poly-Si films was measured using a Digital Instrument atomic force microscope (AFM) with oscillating cantilever operating in “tapping mode.” The spatial resolution of the AFM using etched Si tips was on the order of 5 nm. X-ray microprobe analysis was also performed on poly-Si films prior to and after laser processing using a JEOL JSM 840 scanning electron microscope with x-ray energy up to 10.2 keV. For 0.55 μm poly-Si film thickness we used a 4 keV electron beam setting, which would exhibit a 0.4 μm electron penetration depth in Si single crystal. Therefore, the x-ray response from the glass or quartz substrate is negligibly small.

The PL spectra at three temperatures are shown in Fig. 1 for poly-Si films deposited at 625 °C. At 4.2 K two distinctive luminescent bands at 0.9 and 0.65 eV were clearly observed. No other PL transitions were detected at a higher energy up to poly-Si band gap. The 0.9 eV band was previously identified as due to recombination of electrons and

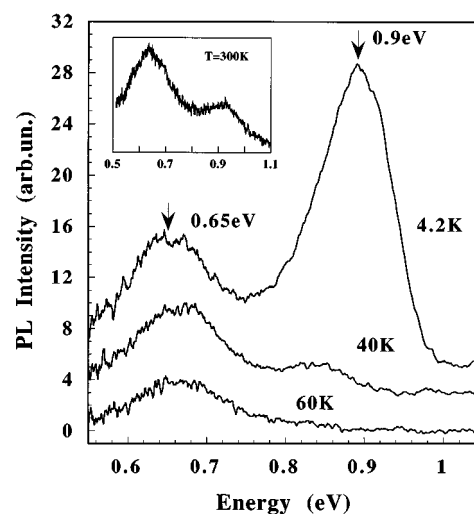


FIG. 1. Photoluminescence spectra at different temperatures in poly-Si thin films deposited at 625 °C. PL was excited by Ar laser 514 nm line with power density of 3 W/cm^2 , and detected with PbS. In the inset, room-temperature PL of the same sample excited by focused laser beam (density of power 300 W/cm^2).

^{a)}Electronic mail: ostapenko@cmd.usf.edu

^{b)}On leave from Institute of Semiconductor Physics, Academy of Sciences, pr. Nauki 45, Kiev 252028, Ukraine.

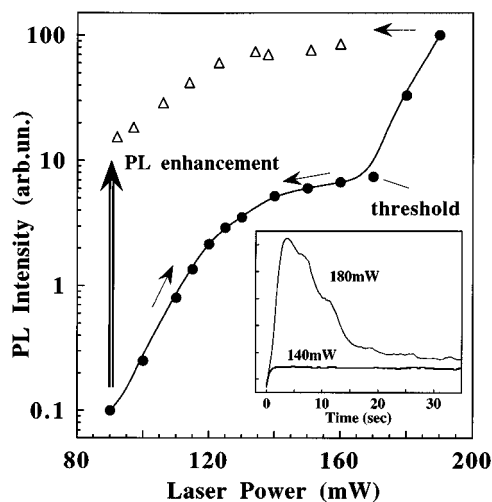


FIG. 2. Intensity dependence of room-temperature luminescence vs excitation laser power ($h\nu_{\text{PL}}=0.73$ eV). Threshold laser power is about 175 mW. Arrows show the increasing and decreasing of laser power. Inset: PL kinetics under subthreshold excitation with 140 mW laser power and with 180 mW above-threshold excitation.

holes trapped in the conduction and valence band-tail states in poly-Si.⁴ With increasing temperature, this band-tail luminescence is strongly shifted to lower energy and quenched as a result of thermal ionization of electrons and holes captured to shallow band-tail states. To the contrary, the 0.65 eV “defect” PL band maintained its maximum position from 4.2 to 300 K, and sustains at room temperature (Fig. 1, inset). We note that this defect PL band is very similar to the oxygen related room-temperature luminescence previously observed in Cz-Si annealed at 470 °C for 64 h.⁵

With increased laser excitation power W_{ex} , the defect PL band intensity I_{PL} , shows a superlinear dependence at room temperature (Fig. 2). This dependence of I_{PL} vs W_{ex} is entirely reversible until the threshold value of laser power (175 mW in the present case) is achieved. This value of threshold energy corresponds to about 55 kW/cm² power density of focused beam. By exceeding this threshold, we found a rapid increase of PL intensity by exposing a film for a few seconds with the Ar⁺ laser. Following this above threshold exposure, the I_{PL} vs W_{ex} dependence was no longer reversible, but rather exhibited a strong hysteresis as shown in Fig. 2. It results to PL enhancement at low laser power excitation, which is characterized by the following. (a) The maximum PL enhancement occurs within 2–10 s (Fig. 2, inset) with above threshold exposure. Shorter exposure time corresponds to higher laser power density. PL enhancement is followed by a strong luminescence quenching with laser exposure longer than 10 s. The last process is related to film damaging as observed with AFM. In Fig. 2 (inset) we show two PL kinetics with below threshold and above threshold laser excitation. (b) The enhancement ratio, $\rho = I_{\text{PL}}$ (after annealing) / I_{PL} (before annealing), measured at low excitation power (90 mW) ranges from 10 to 150 in different samples. This value depends on a type of substrate (quartz or glass), film deposition temperature (550 or 625 °C), and ambient gas during annealing (dry air, oxygen, or nitrogen) compared to vacuum. (c) By varying exposure time

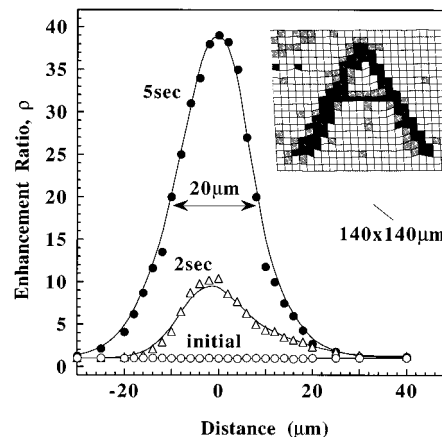


FIG. 3. Line scans of room-temperature PL ($h\nu_{\text{PL}}=0.73$ eV) across the laser annealed point at $x=0$ with different exposure time. Above-threshold laser power of 180 mW was used for annealing. Inset: room-temperature PL micropattern ($140 \times 140 \mu\text{m}$) obtained by laser annealing technique. The character “A” width is about $20 \mu\text{m}$. The average contrast ratio of PL map is ~ 6 .

we observed a gradual increase of PL enhancement measured at the same annealed spot. This is shown in Fig. 3 as line scans across the point with $x=0$, where the laser hits poly-Si. The increased PL intensity shows a maximum with a half-width of about $20 \mu\text{m}$ corresponding to the spot size of the focused Ar-laser beam.

By using atomic force microscopy, we found that PL enhancement is accompanied by surface topography modification of poly-Si films. In Fig. 4(a) we present the AFM map of a laser annealed poly-Si area with about 10 times PL enhancement. One can see in the $20 \mu\text{m}$ laser annealed spot that relatively large polycrystalline grains with the grain diameter exceeding $1 \mu\text{m}$ have been produced. This is shown in Fig. 4(b) using cross-section analysis. This grain size can be compared with poly-Si grains in a nonannealed region of the film which ranged from 80 to 150 nm. These AFM data demonstrate that grain-size enlargement of poly-Si film occurs with Ar laser annealing.

High-power laser processing (700 kW/cm^2) leading to increasing grain size by a factor of two orders of magnitude is well-documented in poly-Si thin films deposited on the Si/SiO₂ substrate.⁶ Poly-Si film recrystallization due to pulsed excimer laser annealing is responsible for the improvement of thin-film transistor characteristics on SiO₂/glass substrates.⁷ In particular, electron mobility in laser recrystallized films can be increased by a factor of ten. We have revealed an additional benefit of laser anneal film processing as the enhancement of room-temperature luminescence. To the contrary of Si wafers, a relatively low thermal conductivity of glass and quartz substrates promotes a reduction by a factor of two orders of magnitude of the Ar-laser power density. A further advantage of poly-Si on glass annealing is that the effect is strongly localized. This is demonstrated in the inset of Fig. 3, where the micropattern of the letter “A” (selectively laser exposed area of poly-Si) is shown as $140 \times 140 \mu\text{m}$ PL map with the character linewidth of about $20 \mu\text{m}$. The average contrast of luminescence pattern corresponds to $\rho=6$.

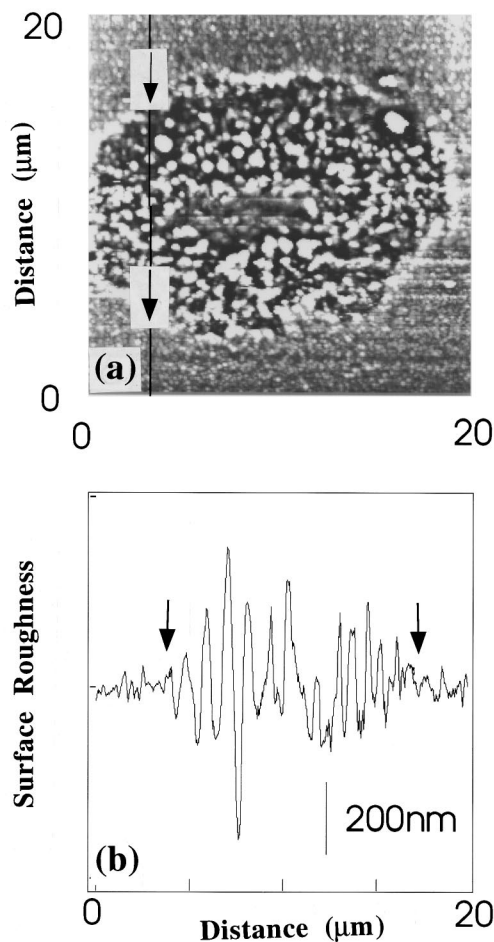


FIG. 4. (a) Surface topography of the laser annealed spot in poly-Si on quartz substrate measured with atomic force microscope, (b) increasing of surface roughness in laser annealed film area. Markers at (a) and (b) depict the same sample points.

We may argue that the oxygen is incorporated into poly-Si due to laser processing. (1) Using electron microprobe x-ray analysis, we found that the silicon peak at 1.74 keV and oxygen peak at 0.54 keV are observed in laser annealed film areas. This can be compared to x-ray spectrum of nonannealed films, where only the silicon peak was found. This is direct evidence that oxygen is incorporated into laser annealed areas of poly-Si films. (2) According to published data, oxygen-related luminescence similar to our 0.65 eV PL band was observed after 450 °C heat treatment in Cz-Si.⁵ Furthermore, we observed that the initial rate of 0.65 eV PL band enhancement (first seconds of laser annealing) is higher than that for 0.9 eV band-tail luminescence. Therefore, we may suggest that oxygen defects are introduced into poly-Si film at the initial steps of laser processing. (3) In some cases, the additional PL band at 0.8 eV occurred in laser annealed areas. This 0.8 eV band is clearly observed in our poly-Si samples subjected to oxygen plasma treatment, and has been previously attributed to oxygen precipitates.⁸ (4) We performed laser annealing in various ambient gases (dry air, oxygen, nitrogen, helium) in addition to vacuum annealing. The vacuum laser annealing using HF dipped samples have shown the presence of PL enhancement. The effect is independent on ambient air pressure from 0.1 to 10^{-5} Torr.

Therefore, we may conclude that film oxygenation from the surface is negligibly small. Laser annealing performed in the dry air or pure oxygen ambient exhibited a stronger PL enhancement compared to vacuum. In particular, the oxygen pressure of about 1 atm increases the maximum ρ value by a factor of two with respect to ρ in vacuum annealed spots and makes the area of PL enhancement more localized. The oxygen ambient also facilitates the anneal kinetics by reducing almost twice the exposure time needed to approach a maximum ρ value.

Based on our findings we conclude that luminescence enhancement in poly-Si thin films is accompanied by two distinctive processes: (1) the increase of grain sizes due to poly-Si film recrystallization exhibited by AFM topography, and (2) oxygen incorporation into annealed areas from the substrate (glass, quartz) or/and from the ambient gas. It is recognized that the grain boundary defects in polycrystalline materials generate nonradiative recombination centers, which eventually reduce luminescence efficiency. There are two possibilities to diminish their role as recombination centers exhibited as a dramatic increase of PL intensity: by poly-Si film passivation produced by a hydrogenation film processing,⁴ or by reducing the grain boundary volume due to an increase in grain size.⁶

The observation of relatively strong luminescence in poly-Si thin films can be accounted for by a presence of tail states close to the conduction and valence band.⁹ The electron and hole capture into band-tail states has a high probability due to wave function delocalization of shallow band-tail states. This initial carrier capture is followed by a thermalization of trapped electrons and holes by emitting acoustic phonons until carriers approach deepest band-tail states. At this point, thermalized carriers can radiatively recombine giving rise to luminescent band-to-band or band-to-center transitions. The electron-hole tunneling recombination of captured carriers is a very efficient mechanism of luminescence. We can suggest that laser annealed poly-Si films on low-cost glass substrates can be a promising material for a new type of electroluminescent devices integrated with Si technology.

We would like to acknowledge helpful discussions with J. Siejka and M. Tajima and the technical assistance of E. I. Oborina. This work was supported by Grant No. MDA972-92-J-1033 from Advanced Research Projects Agency.

¹G. Davies, Phys. Rep. **176**, 83 (1989).

²D. G. Hall, Mater. Res. Soc. Symp. Proc. **298**, 367 (1993).

³O. King and D. G. Hall, Phys. Rev. B **50**, 10661 (1994).

⁴A. U. Savchouk, S. Ostapenko G. Nowak, J. Lagowski, and L. Jastrzebski, Appl. Phys. Lett. **67**, 82 (1995).

⁵M. Tajima, J. Cryst. Growth **103**, 1 (1990).

⁶K. F. Lee, T. J. Stultz, and J. F. Gibbons, in *Semiconductors and Semimetals* (Academic, New York, 1984), Vol. 17, p. 227.

⁷H. Kuriyama, S. Kiyama, and S. Noguchi, et al., Jpn. J. Appl. Phys. **30**, 3700 (1991).

⁸M. Tajima, H. Takeno, M. Warashina, and T. Abe, in *Defects in Semiconductors 17*, edited by H. Heinrich and W. Jantsch (Trans Tech, Switzerland); Mater. Sci. For. **143-147**, 147 (1994).

⁹J. Werner and M. Peisl, Phys. Rev. B **31**, 6881 (1985).